PCCP

PAPER

View Article Online
View Journal | View Issue

Cite this: *Phys. Chem. Chem. Phys.*, 2016, **18**, 9554

Hydrogen bonding in DPD: application to low molecular weight alcohol–water mixtures†

Gokhan Kacar*[abc] and Gijsbertus de With*[a]

Received 1st February 2016,
Accepted 9th March 2016

DOI: 10.1039/c6cp00729e

www.rsc.org/pccp

In this work we propose a computational approach to mimic hydrogen bonding in a widely used coarse-grained simulation method known as dissipative particle dynamics (DPD). The conventional DPD potential is modified by adding a Morse potential term to represent hydrogen bonding attraction. Morse potential parameters are calculated by a mapping of energetic and structural properties to those of atomistic scale simulations. By the addition of hydrogen bonding to DPD and with the proposed parameterization, the volumetric mixing behavior of low molecular weight alcohols and water is studied and experimentally observed negative volume excess is successfully predicted, contrary to the conventional DPD implementation. Moreover, the density-dependent DPD parameterization employed provides the asymmetrical shapes of the excess volume curves. In addition, alcohol surface enrichment at the air interface and self-assembly in the bulk is studied. The surface concentrations of alcohols at the air interface compare favorably with the experimental observations at all bulk-phase alcohol fractions and, in consonance with experiment, some clustering is observed.

Introduction

Coarse-grained simulations have become useful tools to study the temporal evolution and equilibrium properties of soft fluid particles at time and length scales that are not feasible by atomistic simulations.[1] Coarse-graining, by definition, is grouping atoms together based on their chemical functional groups and forming beads. By coarse-graining of a particular molecule, its behavior at longer times and at larger length scales can be simulated. Within the coarse-grained simulation methods, dissipative particle dynamics (DPD) is one of the most widely applied simulation tools to study soft matter.[2] By mapping of coarse-grained parameters to known experimental quantities, such as thermodynamic and transport properties, non-bonded DPD parameters can be calculated.[3] This mapping ensures that the thermodynamic properties are recovered correctly, and a mesoscopic structure is created accordingly. Moreover, the pair-wise nature of interactions conserves the hydrodynamic behavior which is crucial to reach longer time-scales.[4] In the conventional DPD implementation, the interactions are purely repulsive and beads are regarded as soft, interpenetrable particles having molar volumes similar to experimental pure-liquid molar volumes. The assumption of beads having similar volumes has been a limitation in simulating practically relevant polymers as different functional groups may vary largely in volume. Recently, an extension was introduced to parameterize DPD interactions to model beads having variable liquid densities.[5] By this density-dependent parameterization, variable local volumes of beads can be created for a cross-linked polymer.[6]

Although the trade-off between more or less repulsive interactions has been observed to yield the proper structure of soft matter,[7] the repulsive nature of DPD possesses significant drawbacks in predicting the physical properties of liquids. An important example is the volume shrinkage upon mixing of some liquids. The presence of hydrogen bonding[8] in simple alcohol water mixtures, such as methanol–water,[9] ethanol–water[10] and 1-propanol–water[11] results in negative volume excess. The repulsive DPD potential always predicts positive volume excess and is therefore not useful to predict the mixing behavior of liquids. Moreover, the consideration of hydrogen bonding in DPD is implicit as the interactions are read from the Flory–Huggins parameters which are directly related to the solubility parameters.[12] Based on the Hansen approach, a solubility parameter is calculated by adding dispersion, dipolar, and hydrogen bonding contributions.[13] This means that hydrogen bonding in the solubility approach increases the repulsive interaction strength between beads. Volume shrinkage upon mixing can only be realized as attraction arising from hydrogen bonding is implemented properly in DPD. Moreover, explicit

[a] *Laboratory of Materials and Interface Chemistry, Department of Chemical Engineering and Chemistry, Eindhoven University of Technology, Eindhoven, The Netherlands. E-mail: g.dewith@tue.nl*
[b] *Dutch Polymer Institute (DPI), P.O. Box 902, 5600 AX Eindhoven, The Netherlands*
[c] *Department of Genetics and Bioengineering, Faculty of Engineering, Trakya University, 22030, Edirne, Turkey. E-mail: gokhankacar@trakya.edu.tr*

† Electronic supplementary information (ESI) available: Further details on mapping of D_0 from atomistic simulations, fitting of α and DPD simulation parameters. See DOI: 10.1039/c6cp00729e

addition of the hydrogen bonds would yield benefits, such as monitoring formation and breaking of hydrogen bonds, estimating the total hydrogen bond energy contribution, controlling the hydrogen bond formation conditions (*e.g.*, switching on/off), to estimate its effect on the structure of the liquid.

In this work, hydrogen bonding is implemented in DPD by adding a Morse potential term to the conservative DPD potential. A similar approach is reported previously where DPD simulations are used to mimic the helical formation of proteins[14] and where the Morse potential parameters to represent the hydrogen bond attraction are selected arbitrarily. Our work differs from the literature by proposing a realistic parameterization approach to mimic the hydrogen bonding at the DPD level to predict experimentally measured liquid properties.

We first report on the parameterization of the added attractive contribution to the non-bonded potential. Thereafter, we present simulation results with the modified DPD potential and compare them with the experimental volumetric behavior for three sample mixtures: methanol–water, ethanol–water, and 1-propanol–water. Finally, we demonstrate interfacial alcohol enrichment at the air interface, and compare this behavior for those systems with experimental data.

Methods and computational details

Details of DPD simulations

DPD is a coarse-grained simulation method where all the non-bonded interactions conventionally are repulsive. The molecular functional groups are represented in terms of larger entities, usually denoted as beads. The total force $\vec{f}^{\,T}$ acting on a particular bead in DPD is represented by three forces: conservative $\vec{f}^{\,C}$, random $\vec{f}^{\,R}$, and dissipative $\vec{f}^{\,D}$.[3]

$$\vec{f}^{\,T} = \vec{f}^{\,C} + \vec{f}^{\,R} + \vec{f}^{\,D} \quad (1)$$

The thermostating in the simulations is maintained by coupling between the dissipative and random forces, that are acting pair-wise and thus preserve momentum.[3] The conservative force represents the interactions that are soft and determine the equilibrium structure. The conservative potential has the form

$$V_{\mathrm{DPD},ij}(r) = \begin{cases} \frac{a_{ij}}{2}\left(1 - \frac{r}{r_{\mathrm{DPD}}}\right)^2 & r < r_{\mathrm{DPD}} \\ 0 & r \geq r_{\mathrm{DPD}} \end{cases} \quad (2)$$

where r_{DPD} is the interaction cut-off, r is the distance between beads i and j, and a_{ij} is the maximum repulsion in $k_{\mathrm{B}}T$ units. The value of r_{DPD} corresponds with the value of a DPD unit length and is calculated as 4.48 Å by taking a single bead equal to the size of a water molecule from $\rho_{\mathrm{water,pure}} {r_{\mathrm{DPD}}}^3 = 3$.

The usual mapping of DPD parameters a_{ij} from experimental properties is provided by the relation $\Delta a_{ij} = C \times \chi_{ij} k_{\mathrm{B}}T$ between beads i and j, where χ_{ij} is the Flory–Huggins parameter[12] and Δa_{ij} is the excess repulsion. The proportionality parameter C changes as a function of number density.[3] In our simulations, we use an alternative parameterization where beads are represented by variable volumes *via*[5]

$$a_{ij} = \hat{a}_{ij} + \frac{p}{0.0454\left(a_{ii}\rho_{i,\mathrm{pure}} + a_{jj}\rho_{j,\mathrm{pure}}\right)}\chi_{ij}k_{\mathrm{B}}T, \hat{a}_{ij} = \sqrt{a_{ii}a_{jj}},$$

$$\text{with } a_{ii} = \frac{p - \rho_{i,\mathrm{pure}}k_{\mathrm{B}}T}{\alpha {\rho_{i,\mathrm{pure}}}^2 {r_{\mathrm{DPD}}}^3} \quad (3)$$

where a_{ii} and a_{jj} are the self-repulsive interactions, $\hat{a}_{ij}$ is the neutral interaction parameter, ρ_i is the dimensionless number density of the pure components and α is the scaling relation between the excess pressure and the number density. With this parameterization the local densities are properly modeled during simulations.[6]

The scaling function α is a constant for $\rho {r_{\mathrm{DPD}}}^3 > 3$ and equal to 0.101, as reported in Groot and Warren's original work.[3] However, in our simulations the dimensionless number densities of individual beads does not correspond to 3. This means that the excess local pressure created by bead i at the density ρ_i might be different than for bead j at ρ_j. This violates the condition of mechanical equilibrium between different beads (see, eqn (3)). Therefore, we remove the effect of low-density on excess pressure by evaluating α at different densities. A polynomial of order three is fitted to Groot and Warren's α data (Fig. 4 of ref. 3) and α is calculated from this fit (see, Fig. S1 in ESI†). The calculated α is used in eqn (3) to compute a_{ii}.

Hydrogen bonding in DPD

To mimic the attraction due to the presence of hydrogen bonds upon contact of the corresponding hydrogen bonding pairs, a Morse potential term is added to the conservative potential of DPD. A Morse potential has the general form

$$V_{\mathrm{Morse}} = D_0[\mathrm{e}^{-2\sigma(r-r_0)} - 2\mathrm{e}^{-\sigma(r-r_0)}], \quad r < r_{\mathrm{DPD}} \quad (4)$$

where D_0 characterizes the depth of the potential well, σ the width of the potential, and r_0 the equilibrium distance of the hydrogen bonds. We take the value of σ as $2/r_{\mathrm{DPD}}$ and hydrogen bond interactions are considered within a radius of $1r_{\mathrm{DPD}}$, similar to the rest of the non-bonded interactions.

In general, hydrogen bonds are directional, meaning that a particular angle between acceptor, donor and hydrogen atom provides the optimal attraction. However, in DPD simulations, we do not consider an angle term in the Morse potential. There are two reasons for this assumption: (1) coarse-grained beads lack atomistic detail. Therefore, the exact locations of hydrogen, acceptor and donor atoms are not known, and the angle constraint cannot be specified. (2) DPD time in physical units is comparable or larger than the typical dissociation time of hydrogen bonds. The unit time in DPD is often calculated by mapping the dynamic properties to real quantities. For example, Groot and Rabone calculated the DPD unit time by mapping the diffusion coefficient of water as calculated in DPD simulations to experimental values. They obtained a DPD unit time of about 90 ps.[15] In reality, hydrogen bonds dissociate within 1–6 ps.[16]

Therefore, it is reasonable to assume that the directionality of hydrogen bonding is averaged out.

Details of DPD simulations

DPD simulations are run with the LAMMPS simulator[17,18] by using an *NPT* ensemble with the pressure set to $25.73k_BT/r_{DPD}^3$ and the temperature to unity. The pressure is controlled in all dimensions of the box. The simulation box dimensions are $x = 20r_{DPD}$, $y = 20r_{DPD}$, $z = 20r_{DPD}$ and contains 24 000 beads, corresponding to an average number density of 3. The total duration of each simulation is 1×10^6 time-steps with the first 2×10^5 time-steps for equilibration and the rest for data collection. The time step in the simulations is selected as $\Delta t = 0.02t_{DPD}$. Periodic boundary conditions are employed in all dimensions. Hydrogen bonding interactions are switched-on following the equilibration of mixtures.

For the surface composition simulations, air is introduced as a random structure with a high number density of $15r_{DPD}^3$ in order to prevent the liquid penetration to air. The number of air beads corresponds to 24 000. The air beads are fixed at their positions at all times of the simulation with DPD like-like interactions of $10k_BT$ and pair-wise interactions with the alcohols and water of $300k_BT$. These parameters are set arbitrarily as we are interested in the relative concentration differences rather than the exact structure at the interface.

Details of MD simulations

Simulation boxes representing the alcohol–water liquid mixtures are simulated with the Materials Studio package[19] using the COMPASS force field.[20] Different molar ratios are used with 200 molecules. This corresponds to a box size of about 20 Å × 20 Å × 20 Å. Initially, simulation boxes are energy minimized, and then *NPT* simulations are performed for 1 ns to reach the equilibrium density at a temperature of 25 °C. Next, *NVT* simulations are run at the equilibrium liquid mixture density for another 1 ns. For temperature and pressure control, the Nosé–Hoover thermostat[21–24] and the Berendsen barostat[25] with a decay constant of 0.1 ps are used, respectively. The simulation output is analyzed and averaged for the final 500 ps of the *NVT* run.

Results and discussion

The strength of the hydrogen bond attraction is reflected by D_0 parameter in the Morse potential. The parameter D_0 is referred as the effective mixing energy and represents mainly ''hydrogen bonding'' energy. By computing the ''effective energy'' we explicitly treat the hydrogen bonding interactions as many-body interactions acting on a particular hydrogen bonding bead. Therefore, our approach can be seen as a solution procedure similar to the conventional DPD parameterization. The procedure we propose is different from the usual one in the MD practice of modeling hydrogen bonds and we do not expect right away a match in between the hydrogen bond strength as computed from MD simulations and our computed energies. The reason is that in a MD force field, parameterization of only a single hydrogen bonding pair is made as a result of, say, Lennard-Jones and electrostatic interactions. Moreover, quantifying the hydrogen bonding energy in MD simulations refers to defining an angle and a distance between the acceptor and donor atoms and computing the hydrogen bond energy within a pre-defined cut-off distance. However, as mentioned before, we do not explicitly consider an angular dependence.

We target to obtain D_0 from physical quantities. One approach to calculate D_0 is to perform atomistic level simulations for each mixture. In this way, the effective hydrogen bond interaction strength can be constructed between alcohol and water molecules avoiding the directionality constraint. The effective strength for each mixture is quantified for 1 mole by using the standard energy difference method[26,27]

$$D_0(x) \equiv E_{\text{H-bond}}(x) = E_{\text{Pot,Mix}}(x) - E_{\text{Pot,A}} - E_{\text{Pot,W}} \quad (5)$$

where $E_{\text{H-bond}}$ is the strength of the hydrogen bond, $E_{\text{Pot,Mix}}$ is the potential energy of the alcohol–water mixture and $E_{\text{Pot,A}}$ and $E_{\text{Pot,W}}$ are the potential energies of alcohol and water at their pure state, respectively. In the study of Wensink *et al.*,[28] the intermolecular energies E_{inter} of the same alcohol–water mixtures at different concentrations were calculated from a series of MD simulations. The potential energy can be identified as

$$E_{\text{Pot}}(N_W + N_A) = (N_W + N_A)E_{\text{inter}} + N_W E_{\text{intra,W}} + N_A E_{\text{intra,A}} \quad (6)$$

where $E_{\text{intra,W}}$ and $E_{\text{intra,A}}$ are the intramolecular energies, N_W and N_A are the number of molecules corresponding to water and alcohol in the mixtures, respectively. We adopt the values of $E_{\text{intra,W}}$ and $E_{\text{intra,A}}$ from their work.[28]

Having D_0 calculated, the r_0 values are estimated from the radial distribution functions (RDFs) as these functions characterize the amount of neighboring hydrogen bonding pairs. For this purpose, series of Molecular Dynamics (MD) simulations were performed and the RDFs between the center-of-mass (CoM) of the hydrogen bonding molecules, namely the alcohols and the water, were computed. The results are shown in Fig. 1.

In principle, the location of the minima between the first and the second peak of the RDF gives the non-bonded separation distance. This distance is about $0.70r_{DPD}$ for the three alcohol–water mixtures. In our proposed parameterization, this value constitutes the initial value for iteration to determine the absolute values for r_0 used in DPD simulations. The trial r_0 values are varied between $0.60r_{DPD}$ and $0.80r_{DPD}$ and the values that give the proper estimates for the negative volume excess values are selected. For the sake of comparison, the typical separation of the CoM of two water molecules at its pure-liquid state is about $0.67r_{DPD}$.[29] As shown in Table 1, setting a single r_0 value in the Morse potential for methanol–water and ethanol–water mixtures is sufficient to account for the hydrogen bond attraction. However, for the 1-propanol–water mixture, a wider distribution of r_0 values with respect to the changing concentration difference should be incorporated in order to mimic the volumetric properties. This is also in line with the results for the RDFs in Fig. 1. For the methanol and ethanol mixtures, we

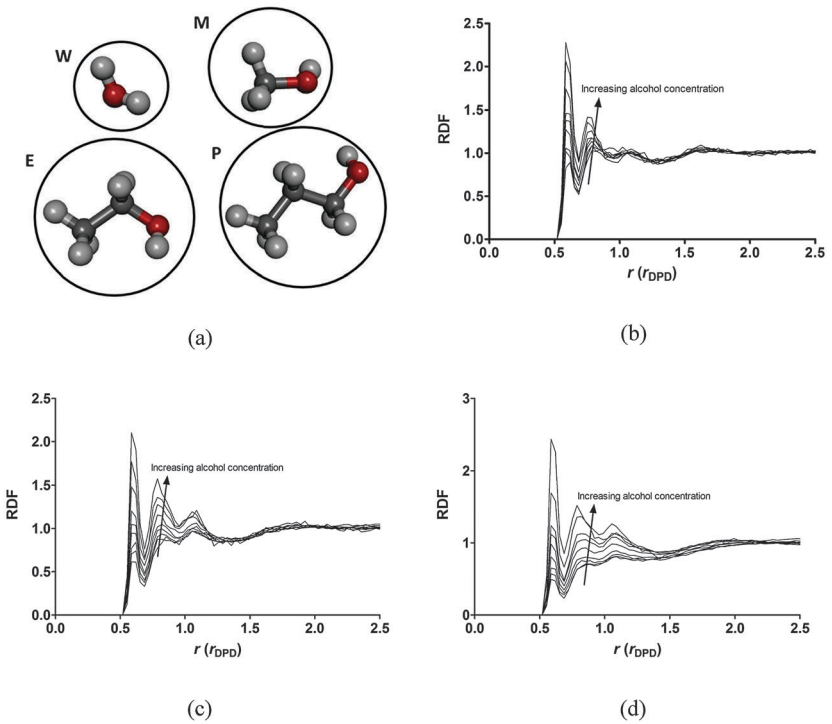

Fig. 1 (a) The coarse-graining of water (W), methanol (M), ethanol (E) and 1-propanol (P). RDF plots of alcohol–water beads in (b) methanol–water, (c) ethanol–water and (d) 1-propanol–water. RDFs are calculated from MD simulations but presented in DPD units for convenience.

Table 1 Effective hydrogen bond strength D_0 and equilibrium distance of hydrogen bonds r_0 for methanol–water, ethanol–water and 1-propanol–water mixtures for different concentrations

	Methanol–water		Ethanol–water		1-Propanol–water	
$x_{alcohol}$	D_0 [k_BT]	r_0 [r_{DPD}]	D_0 [k_BT]	r_0 [r_{DPD}]	D_0 [k_BT]	r_0 [r_{DPD}]
0.10	5.06	0.78	8.22	0.78	7.21	0.60
0.20	6.33	0.78	9.14	0.78	8.28	0.69
0.30	7.46	0.78	9.97	0.78	9.23	0.73
0.39	8.68	0.78	10.85	0.78	10.25	0.75
0.51	10.07	0.78	11.86	0.78	11.42	0.77
0.59	11.12	0.78	12.62	0.78	12.30	0.77
0.69	12.41	0.78	13.56	0.78	13.38	0.78
0.84	14.20	0.78	14.86	0.78	14.88	0.78
0.93	15.31	0.78	15.66	0.78	15.82	0.78

observe a relatively narrow distribution of neighboring shells, while for the 1-propanol mixture the distribution is much wider. Moreover, the directionality of the beads is not taken into account in DPD simulations. Therefore, the separations between the CoMs of the hydrogen bonding pairs (in our case r_0s) are different in the DPD simulations from those in the MD predictions.

A comparison of the calculated hydrogen bond strengths can be made with the hydrogen bonds in water. The total strength of attraction between water molecules in the liquid state has been reported as 23.3 kJ mol^{-1}.[30] Assuming, on average, a tetrahedral arrangement and pair-wise interactions,[31] per hydrogen bond the energy value is about 6 kJ mol^{-1}, equal to $2.4k_BT$.

For the sake of comparing experimental and simulation results, the excess volume V^E is calculated from the product of the molar fraction x_i, liquid density of the mixture ρ_L, molar volume V_i, and molecular weight M_i of each component i. In our notation components i represent alcohol A and water W, *i.e.*,

$$V^E = \frac{x_A M_A + x_W M_W}{\rho_L} - x_A V_{m,A} - x_W V_{m,W} \qquad (7)$$

where V^E is equivalent to the difference in the actual volume and the ideal volume of the mixture. In the right-hand-side of eqn (7), the first term represents the volume of mixture and the last two terms represent the volume of the ideal mixture. The comparison between the results of the simulations and the experiments is made by considering the fractional volume change of the mixtures, calculated by dividing the excess volume by the ideal contribution (see, Fig. 2).

Fig. 2 depicts that conventional DPD simulations are not able to capture the volume change upon mixing of different alcohol-water mixtures. As expected, a volume increase is observed. Mimicking hydrogen bonds by adding a Morse potential in DPD clearly leads to volume shrinkage upon mixing of alcohol and water with a good match between the simulation and experimental results. Besides, the increasing asymmetry in the shape of the curves, as observed experimentally as a function of the molecular weight of the alcohol, is reproduced properly. Here the DPD simulations lead to asymmetric curves as a result of the alternative DPD parameterization[5] in which the differences in bead volumes are taken into account, while the conventional DPD parameterization results in symmetric curves.

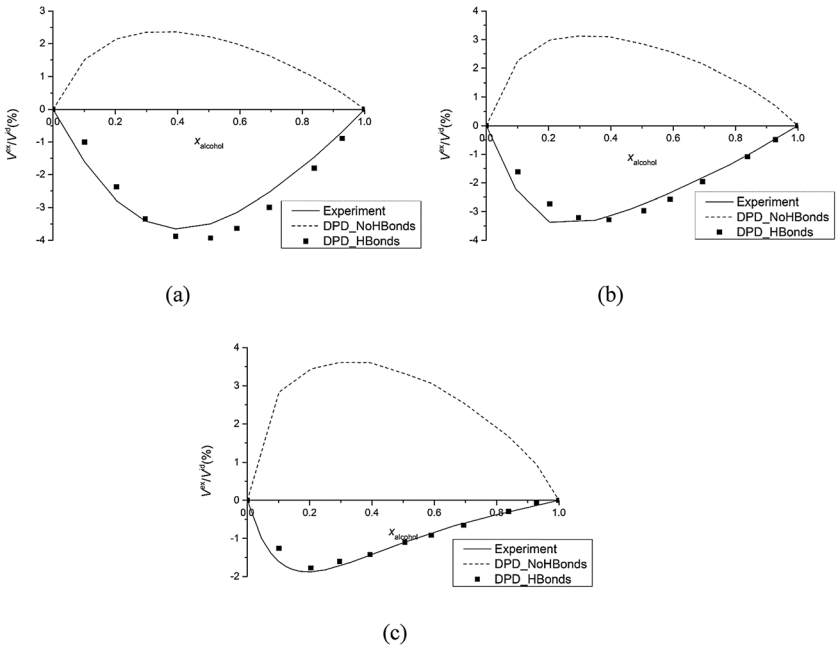

Fig. 2 Fractional volume changes of (a) methanol–water, (b) ethanol–water and (c) 1-propanol–water upon mixing estimated from DPD simulations (filled squares) and compared to experimental data (solid line) and to the DPD simulations without taking hydrogen bonds into account (dashed line).

Experimentally, for an air interface near the alcohol–water mixture, the interface is known to be enriched in alcohol.[32] To verify that the proposed parameterization is capable of predicting this alcohol enrichment, we simulated mixtures including an air interface. At all alcohol molar fractions, alcohol enrichment, as indicated by the surface composition x_{alcohol}(surface), is clearly visible (Fig. 3). While we observe a very good fit for the methanol–water case, for the higher molecular weight alcohols

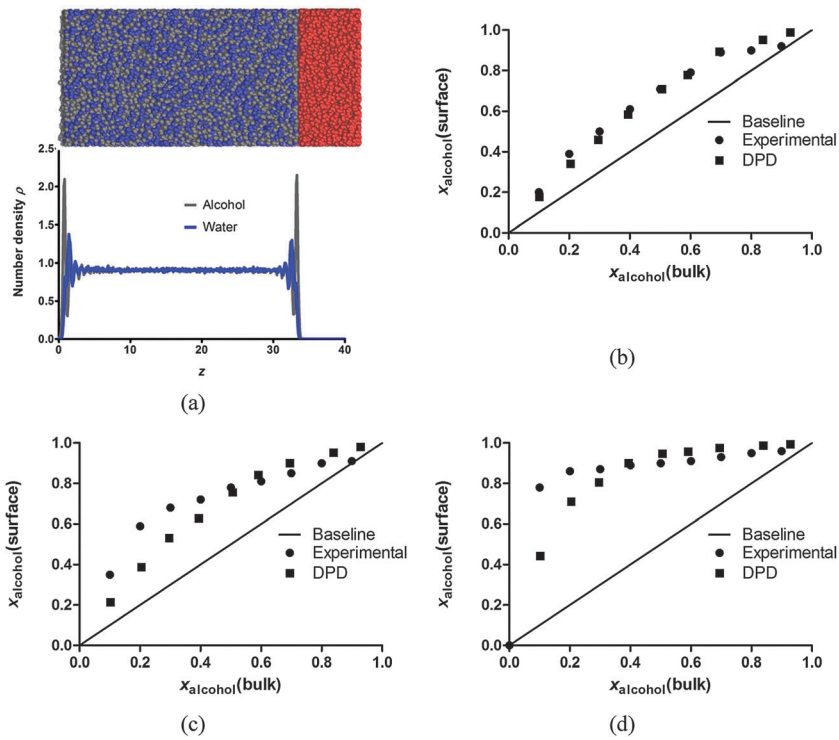

Fig. 3 (a) A representative density profile and snapshot of ethanol–water mixture near the air interface. Simulated (squares) and experimentally observed (circles) (data from ref. 32) alcohol fractions are plotted near the air interface with respect to the bulk fraction of (b) methanol–water, (c) ethanol–water and (d) 1-propanol–water mixtures. The baseline represents a line with slope 1 as a guide for the eye.

the deviation increases at lower alcohol fractions. The length of the hydrophobic tail of 1-propanol is obviously different from that of the methanol molecule, which influences the hydrophilic–hydrophobic balance. Moreover, the coarse-graining is done by taking the whole molecule as a single entity. Therefore, as the alcohol molecular weight increases, the hydrophobic–hydrophilic balance within a single alcohol molecule gradually changes. This might lead to a deviation from the experimental curve since the surface excess also depends on the specific orientation of the hydrophobic part of the alcohol molecules. However, the increasing skewness of the curve for x_{alcohol}(surface) from methanol–water *via* ethanol–water to 1-propanol–water mixture is predicted successfully. Note that the DPD interactions between the air and the liquid mixtures are not tuned to represent their interactions. Therefore, a further optimized approach to properly estimate those interactions is required for a better prediction of experimental observations. This is beyond the scope of the present work. Nevertheless, the experimental behavior is reasonably described.

Table 2 Coordination numbers (CNs) computed for alcohol–alcohol (AA), alcohol–water (AW) and water–water (WW) pairs

	CN				First minimum in RDF		
Alcohol	AA	AW	WW	$C_{\max}$[a]	AA	AW	WW
Methanol	8.8	7.9	4.8	0.5	1.25	1.15	1.05
Ethanol	6.9	9.9	6.3	0.3	1.25	1.15	1.05
1-Propanol	4.6	17.7	13.4	0.2	1.35	1.25	1.15

[a] $C_{\max}$ is the concentration of maximum volume excess.

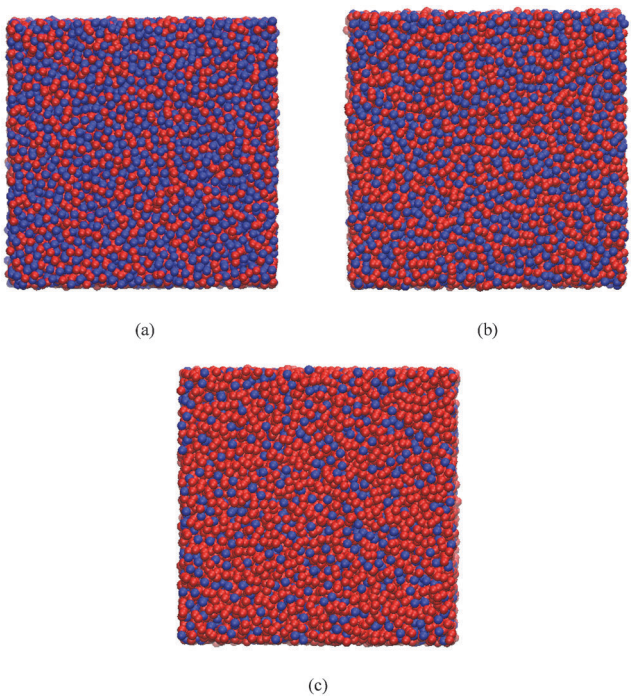

Fig. 4 Snapshots of (a) methanol–water, (b) ethanol–water and (c) 1-propanol–water mixtures for the minimum excess volume concentrations. Alcohols are colored in blue and water are in red.

It is known that water and alcohols are self-assembling fluids and they are able, under some conditions, to give rise to clusters.[33] In Table 2 we show the coordination numbers (CNs) of the water and the alcohol molecules, as calculated from the RDFs of the DPD simulations at the concentration of maximum excess volume ($C_{\max}$).

The table shows that with increasing alcohol molecular weight, the alcohol–alcohol CN decreases while the alcohol–water CN and water–water CN increase. This is, at least partly, due to the decreasing availability of the alcohols as that concentration shift to lower values with increasing alcohol molecular weight. Comparing the alcohol–alcohol CN with the water–water CN, we observe that for methanol the CN is larger than for water, for ethanol the CN is about the same as for water while for propanol it is smaller than for water. This likely partly due to the difference in self-repulsion between the alcohols and water, which renders intrusion of the water beads in between the alcohol beads possible, as also reflected in the RDFs of the mixtures and the increasing alcohol–water CN. The data taken together suggest the presence of clusters of molecules, as has been reported in the literature.[33] In Fig. 4 snapshots of the configurations of the various mixtures at $C_{\max}$ are given. In particular for the methanol and ethanol mixture strings of molecules can be discerned, illustrating clearly the presence of some clustering.

Conclusions

The conventional DPD simulation method lacks the ability to be applied to systems where hydrogen bonding is significant for determining the structure. For example, upon mixing of simple alcohols, such as methanol, ethanol and 1-propanol, with water, volume shrinkage is observed experimentally. Due to the repulsive nature and absence of proper parameterization of hydrogen bonds in DPD, this phenomenon could not be described successfully. Therefore our main message in this work is to report our set up for mimicking attractive hydrogen bonding effects in DPD. We initially demonstrate our proposed procedure to implement hydrogen bonding into DPD. An essential contribution of our work is that the parameters are mapped from physical parameters rather than using arbitrary numbers to represent the system of interest. Hence, the results of atomistic molecular dynamics simulations are used in order to compute the depth of the added hydrogen bond potential and the radial distribution functions to determine the equilibrium hydrogen bond length. As a result of the proposed parameterization, negative excess volumes upon mixing of low molecular weight alcohols and water are predicted successfully. Moreover, the shapes of the excess volume curves are successfully estimated by our density-dependent DPD parameterization. The parameterization procedure is further tested by studying alcohol enrichment at the air interface. Although the DPD parameters considering the interactions with air are set with no mapping from experimental data, the experimentally known alcohol enrichment is predicted correctly. In addition,

the experimentally reported clustering of alcohols is also inferred from the coordination numbers as computed from the RDFs and visible in snapshots of the configuration of the mixtures. In all, the proposed parameterization of DPD for hydrogen bonded systems is shown to describe the experimentally observed physical properties of low molecular weight alcohols properly, thereby enabling the extension of the method to study various systems where hydrogen bonding is of crucial importance, such as biological systems, proteins as well as polymers interacting with water.

Acknowledgements

This research forms part of the research program of the Dutch Polymer Institute (DPI), project #780 'High Heals'. The authors thank Prof. R. A. T. M. van Benthem (DSM/TU/e) for suggesting the use of alcohols for this research.

References

1 S. O. Nielsen, C. F. Lopez, G. Srinivas and M. L. Klein, *J. Phys.: Condens. Matter*, 2004, **16**, R481–R512.
2 P. J. Hoogerbrugge and J. M. V. A. Koelman, *Europhys. Lett.*, 1992, **19**, 155–160.
3 R. D. Groot and P. B. Warren, *J. Chem. Phys.*, 1997, **107**, 4423–4435.
4 P. Español, *Phys. Rev. E: Stat. Phys., Plasmas, Fluids, Relat. Interdiscip. Top.*, 1995, **52**, 1734–1742.
5 G. Kacar, E. A. J. F. Peters and G. de With, *Europhys. Lett.*, 2013, **102**, 40009.
6 G. Kacar, E. A. J. F. Peters and G. de With, *Soft Matter*, 2013, **9**, 5785–5793.
7 G. Kacar, E. A. J. F. Peters and G. de With, *J. Phys. Chem. C*, 2013, **117**, 19038–19047.
8 A. D. Buckingham, J. E. Del Bene and S. A. C. McDowell, *Chem. Phys. Lett.*, 2008, **463**, 1–10.
9 A. Arce, A. Blanco, A. Soto and I. Vidal, *J. Chem. Eng. Data*, 1993, **38**, 336–340.
10 J. P. E. Grolier and E. Wilhelm, *Fluid Phase Equilib.*, 1981, **6**, 283–287.
11 J. V. Herraez and R. Belda, *J. Solution Chem.*, 2006, **35**, 1315–1328.
12 P. J. Flory, *Principles of Polymer Chemistry*, Cornell University Press, Ithaca, New York, 1953.
13 C. M. Hansen, *Hansen Solubility Parameters: A User's Handbook*, CRC Press, Boca Raton, FL, 2007.
14 A. Vishnyakov, D. S. Talaga and A. V. Neimark, *J. Phys. Chem. Lett.*, 2012, **3**, 3081–3087.
15 R. D. Groot and K. L. Rabone, *Biophys. J.*, 2001, **81**, 725–736.
16 F. N. Keutsch and R. J. Saykally, *Proc. Natl. Acad. Sci. U. S. A.*, 2001, **98**, 10533–10540.
17 S. Plimpton, *J. Comput. Phys.*, 1995, **117**, 1–19.
18 S. H. Min, C. Lee and J. Jang, *Soft Matter*, 2012, **8**, 8735–8742.
19 Materials Studio, Accelrys Inc., San Diego, CA, 2014.
20 H. Sun, *J. Phys. Chem. B*, 1998, **102**, 7338–7364.
21 S. Nose, *J. Chem. Phys.*, 1984, **81**, 511–519.
22 S. Nose, *Mol. Phys.*, 1984, **52**, 255–268.
23 S. Nose, *Prog. Theor. Phys. Suppl.*, 1991, 1–46.
24 W. G. Hoover, *Phys. Rev. A: At., Mol., Opt. Phys.*, 1985, **31**, 1695–1697.
25 H. J. C. Berendsen, J. P. M. Postma, W. F. van Gunsteren, A. Dinola and J. R. Haak, *J. Chem. Phys.*, 1984, **81**, 3684–3690.
26 S. F. Boys and F. Bernardi, *Mol. Phys.*, 2002, **100**, 65–73.
27 S. Scheiner, *Hydrogen Bonding: A Theoretical Perspective*, Oxford University Press, New York, 1997.
28 E. J. W. Wensink, A. C. Hoffmann, P. J. van Maaren and D. van der Spoel, *J. Chem. Phys.*, 2003, **119**, 7308–7317.
29 K. Modig, B. G. Pfrommer and B. Halle, *Phys. Rev. Lett.*, 2003, **90**, 075502.
30 S. J. Suresh and V. M. Naik, *J. Chem. Phys.*, 2000, **113**, 9727–9732.
31 P. E. Mason and J. W. Brady, *J. Phys. Chem. B*, 2007, **111**, 5669–5679.
32 G. Raina, G. U. Kulkarni and C. N. R. Rao, *J. Phys. Chem. A*, 2001, **105**, 10204–10207.
33 S. Dixit, J. Crain, W. C. K. Poon, J. L. Finney and A. K. Soper, *Nature*, 2002, **416**, 829–832.

